Heliyon 9 (2023) e19478

Contents lists available at ScienceDirect

Heliyon

journal homepage: www.cell.com/heliyon

Comparative stability study and aggregate analysis of Bevacizumab marketed formulations using advanced analytical techniques

Arpit Arunkumar Bana [a], Nithin Sajeev [b,1], Sabyasachi Halder [b,2], Haidar Abbas Masi [c], Shikha Patel [a], Priti Mehta [a,*]

[a] Department of Pharmaceutical Analysis, Institute of Pharmacy, Nirma University, S. G. Highway, Ahmedabad, 382481, Gujarat, India
[b] Center for Cellular and Molecular Platform (C-CAMP), Bengaluru, 560065, Karnataka, India
[c] Gujarat Biotechnology Research Centre (GBRC), Gandhinagar, 382011, Gujarat, India

ARTICLE INFO

Keywords:
Bevacizumab
Biosimilars
Stress study
Intact mass analysis
Aggregate analysis

ABSTRACT

Bevacizumab (Bvz) is the most preferred recombinant humanized monoclonal antibody in biosimilar development due to its prominence as a standard treatment in the oncology space. Therapeutic monoclonal antibodies are typically more complex and unlikely to produce a replica. As a result, regulatory agencies allow approval of biosimilars that differ structurally and functionally from their reference product, but these differences should not have any clinical significance. To identify these significant discrepancies, it is essential to perform a thorough characterization of critical product attributes both in real-time and after storage until the product's expiration. In the present study, two Bvz biosimilar brands (Bio-1 and Bio-2) marketed in India were evaluated and compared with the reference product Avastin® to assess their degree of similarity. A comprehensive physicochemical characterization of biosimilars and reference product was performed using orthogonal techniques including LC-ESI-QTOF, MALDI-TOF, FTIR-ATR, iCIEF, rCE, nrCE, UV280, and RP-HPLC. Furthermore, Bvz formulations under study were subjected to various stress conditions of thermal (elevated temperature 50 ± 2 °C), chemical (acidic pH 3.0 ± 0.2, neutral pH 7.0 ± 0.2, and basic pH 10.0 ± 0.2), and mechanical (agitation 200 rpm) for comparative stability evaluation. Any alteration in the secondary structure of the native protein was detected and quantified using far-UV circular dichroism (CD), indicating an average of 15% and 11% loss in native antiparallel β-sheet conformation respectively in Bio-1 and

Abbreviations: **Bvz**, Bevacizumab; **Avt**, Avastin®; **Bio-1**, Biosimilar-1; **Bio-2**, Biosimilar-2; **mg/ml**, Milligram per milliliter; **µg/ml**, Microgram per milliliter; **ESI-QTOF**, Electrospray ionization-quadrupole time of flight mass detector; **MALDI-TOF**, Matrix-assisted laser desorption ionization-time of flight mass detector; **FTIR-ATR**, Fourier transform infrared spectroscopy with Attenuated Total Reflectance; **iCIEF**, Imaged capillary isoelectric focusing; **rCE**, Capillary electrophoresis in reduced condition; **nrCE**, Capillary electrophoresis in non-reduced condition; **UV_{280}**, Ultraviolet spectroscopy at 280 nm; **RP-HPLC**, Reversed phase-high performance liquid chromatography; **CD**, Circular dichroism; **SEC-MALS**, Size exclusion chromatography-multi angle light scattering detector; **rpm**, Rotation per minute; **mAbs**, Monoclonal antibodies; **CQA**, Critical quality attributes; **USFDA**, United States Food and Drug Administration; **ICH**, International Council of Harmonization; **MW**, Molecular weight; **M**, Molar; **mM**, Millimolar; **Da**, Dalton; **KDa**, Kilodalton; **NGHC**, Non-glycosylated heavy chain; **HC**, Heavy chain; **LC**, Light chain; **HMW**, High molecular weight aggregates; **LMW**, Low molecular weight aggregates.

* Corresponding author.
E-mail address: drpritimehta@nirmauni.ac.in (P. Mehta).
[1] SCIEX, Defence Aerospace IT Sector, Bengaluru 562149, Karnataka, India.
[2] Syngene International Limited, Biocon Park, Bengaluru 560099, Karnataka, India.

https://doi.org/10.1016/j.heliyon.2023.e19478
Received 15 March 2023; Received in revised form 9 August 2023; Accepted 23 August 2023
Available online 28 August 2023

Bio-2 upon exposure to elevated temperature and high pH. Additionally, covalent or non-covalent aggregates formed as a function of elevated temperature and agitation were quantified using SEC-MALS.

1. Introduction

Therapeutic recombinant monoclonal antibodies (mAbs) are the fastest-growing biopharmaceuticals due to their crucial role in the therapy of serious and chronic disorders, such as inflammatory bowel disease, diabetes, rheumatoid arthritis, and cancer. The use of these biological products has increased during the last few years. A patent cliff and rising demand for these magical cures encourage the development of competitive biosimilars [1].

A biosimilar is "highly similar" to the reference biological product in terms of structure, but not exactly the same. Because mAbs are produced in living systems, there can be heterogeneity between the proposed biosimilar and its innovator product. This heterogeneity could arise from any post-translational modification or any manufacturing process and can ultimately impact the biosimilars anticipated clinical performance [2].

Therefore, it is essential to conduct robust comparative physicochemical characterization of product attributes which are critical to defining a product's identity, quantity, safety, purity, and potency. This characterization of critical quality attributes (CQA) helps to identify any clinically meaningful differences between the proposed biosimilar and the innovator product. A comparative analytical assessment of CQAs including molecular weight (M.W) of the protein, higher order structure (HOS) characterization, and degradation profiles indicating stability are all addressed as physicochemical characterization studies [3]. Moreover, mAbs are highly sensitive to even minute changes in pH, temperature, light exposure, oxidation, freeze-thaw, and agitation in their immediate environment. For instance, agitation, acidic or basic pH, and high temperature all exacerbate the aggregation of mAb therapeutics and promote peptide bond cleavage. In the event of such incompatibility, the parent structure will change, resulting in a loss of product stability and/or clinical performance [4].

Therefore, regulatory agencies around the world highlight the need to perform real time stability studies, force degradation studies, and accelerated stability studies as part of physicochemical characterization to directly compare the stability of the biosimilar formulation with the innovator product [5]. The comparative force degradation study should ideally be carried out under a variety of stress conditions including thermal, chemical, and mechanical stressors, all of which can lead to gradual product degradation during processing, packaging, shipping and handling [1,5].

Besides, the International Council of Harmonization (ICH) guidelines defined to perform stability testing of biotechnological/biological products Q5C, Q5E (guidance on the use of forced degradation studies), Q1A (R2), Q1B (photostability studies), Q6B (degradation during storage), and Q2 (R1) should also be taking into consideration [6]. Despite multiple challenges, the market for biosimilars is growing impressively. Currently, the USFDA has recommended the approval of 39 biosimilars while the EMA in Europe has recommended the approval of 88 biosimilars. Above all others, Bevacizumab (Bvz) biosimilar development and approval rose to prominence in the biosimilar market due to its crucial role in the treatment of a range of cancers and the patent expiry of its innovator Avastin (Avt) [7].

Bvz is an antiangiogenic recombinant humanized monoclonal antibody and is indicated as a first-line treatment for metastatic colorectal cancer, non-squamous non-small cell lung cancer and metastatic breast cancer. The innovator product of Bvz 'Avastin' (Avt) (F. Hoffmann-La Roche AG, Basel, Switzerland) was first authorised by the European Medicines Agency (EMA) in January 2005 and the US Food and Drug Administration (FDA) in February 2004 Up until 2022, approximately 15 Bvz biosimilars are anticipated to be in development worldwide. Out of those 15, 4 were approved in USA and Europe. In India, there are 13 Bvz biosimilars approved up till November 2022 [8].

In present article, real time stability study was performed in marketed Bevacizumab biosimilar products (Bio-1 and Bio-2), and innovator product Avastin® by doing comprehensive analytical assessment of their critical product attributes like intact molecular weight, quantitative determination of native protein, charge and size variants, and higher order structure. Furthermore, forced degradation study of all the products under examination were carried out over the duration of their shelf lives under thermal, chemical, and mechanical stress conditions. The profile of aggregates, other product-related impurities, and any alterations to higher order structure triggered as a function of elevated temperature, varying pH conditions, and agitation were evaluated using advanced analytical techniques like Far-UV CD and SEC-MALS. All analytical techniques employed in the present study, are shown in Table 1 and

Table 1
Analytical tools used for structural characterization and stability evaluation.

Order of Characterization	Analytical Tools
Intact mass analysis	LC-ESI-QTOF MALDI-TOF
Higher Order (Secondary)	FTIR-ATR and Far UV-CD for secondary structure characterization
Product related Substances and Impurities	r and nrCE-SDS, size heterogeneity analysis iCIEF, charge heterogeneity analysis
Protein Concentration estimation	UV_{280} and RP-HPLC method
Aggregate Analysis	SEC-MALS

were selected based on their accessibility, and competence to accurately detect any qualitative and quantitative differences in the intended product attributes.

2. Results and discussion

Before analysis, general properties like composition, colour, clarity, and appearance of formulations for all three Bvz brands were evaluated. All three brands had similar composition with a mentioned label claim of, 100 mg Bevacizumab (rDNA origin), 240 mg α, α-Trehalose Dihydrate, 23.2 mg Monobasic Sodium Phosphate (Monohydrate), 4.8 mg Dibasic Sodium Phosphate (Anhydrous), 1.6 mg Polysorbate 20, and q.s. to 4.0 ml Water for Injection.

Bvz formulations have a shelf life of 2 years. At the time of purchase, Bio-1, Bio-2 and, Avt had 18 months, 20 months, and 17 months of shelf life remaining before expiration. Finally, the purchased formulation of both biosimilar brands, and the innovator product, were observed for the presence of visible particles but were found to be completely transparent, Fig. 1A and B.

2.1. Intact mass analysis

To evaluate post-approval, real time stability of Bvz biosimilar brands, intact mass analysis was performed using LC-ESI-QTOF (Table S1) and MALDI-TOF instruments. Both instruments are used for Bvz intact mass heterogeneity analysis. However, LC-ESI-QTOF has more advantages compared to MALDI-TOF. By using **LC-ESI-QTOF, total ion current chromatogram (TIC) profile, isolated glycoforms molecular weight, summed ion spectra, deconvoluted mass profiles and post-translational modifications present in protein structure can be identified and reported** [9]. On the other hand, **MALDI-TOF gives information regarding intact mass only**. Using LC-ESI-QTOF, Bio-1 and Bio-2 formulations showed a moderate degree of heterogeneity, in correlation to Avt, according to the observed intact mass spectrum. **Similar TIC profiles** were observed for **Bio-1, Bio-2 and Avt formulations** with experimental retention time **(Rt) values of 3.380 ± 0.2 min, 3.378 ± 0.2 min and 3.628 ± 0.2 min as shown in Fig. 2A** (Figs. S1, S2, S3). Summed ion spectra were observed in the **m/z range of 2000 to 4000** with the **highest m/z value of 3108.6713** as shown in Fig. 2B (Figs. S4, S5, S6). Three isoforms that map to the various glycoforms are visible in the zoomed deconvoluted mass spectrum as shown in Fig. 2C (Figs. S7, S8, S9). The most abundant peaks of the deconvoluted mass spectrum correspond to the **experimental mass of 149,168 Da for Bio-1 and Bio-2 formulation, and 149,167 Da for Avt formulation** (Fig. S10). Thus, suggesting the **positive mass shift of + 4 Da (Bio-1), + 4 Da (Bio-2), and + 3 Da (Avt)** from the target mass of 149,164 Da [10].

For Bio-1, Bio-2, and Avt formulations native spectra and charge state appear to be comparable with identical peak patterns that can be attributed to similar glycoform distributions, as shown Table 2. These data show that even with minimal optimization, it is possible to assign a number of the observed subpeaks to known common glycosylation states of IgG1 using the BioConfirm tool, even though the resolution of individual glycosylation state peaks is far from what can be achieved with extensive and optimized sample preparation. For Bio-1, Bio-2 and Avt, the most abundant peak with **percentage areas of 54.8%, 54.97%, and 45.3%** likely represent the antibody with **two G0 nonfucosylated glycan lacking galactose (NGA2) glycosylations**, Fig. 2D. The next common glycosylation with **percentage area of 35.32% (Bio-1), 35.35% (Bio-2), and 29.44% (Avt) was 1*G1/G0**, which involves the addition of a galactose moiety to one of the N-acetylglucosamine termini along with the presence of nonfucosylated glycan lacking galactose. **The third most abundant glycoform (17.05%) exclusive to Avt** was 2*G1 with an experimental MW of 149,484 Da [11]. The fourth most abundant glycoform, 2*G0F (NGA2) was observed in all three formulations with experimental MW of 149,458 Da (Bio-1), 149, 460 Da (Bio-2), and 149,456 Da (Avt). Additional glycoforms (e.g., G0F/G0) along with the loss of C-terminal lysine residue from both heavy chains were also present as minor populations in all three formulations with **experimental MW of 149,055 Da (Bio-1), 149, 055 Da (Bio-2), and 149, 056 Da (Avt)**, as shown in Fig. 2D and Table 2. The intact mass spectrums obtained using MALDI-TOF for Bio-1, Bio-2 and Avt showed **m/z values of 149,785.165 Da, 149,095.979 Da and 149,189.325 Da**, as shown in Fig. 3A.

2.2. Higher order structure characterization

The real time stability of Bio-1 and Bio-2 formulations was also compared to Avt formulation by investigating their secondary

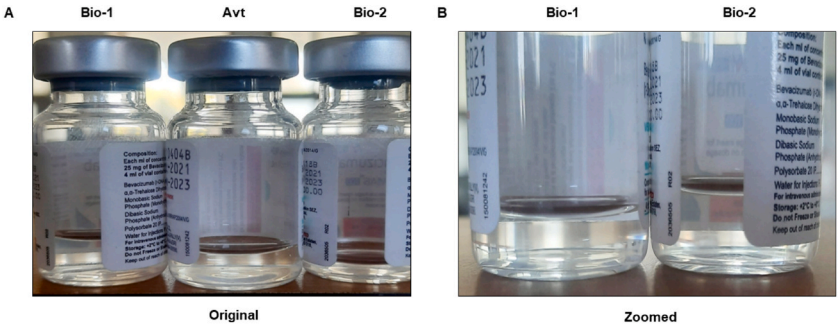

Fig. 1. Image of Bio-1, Bio-2, and Avt vials showing no visible particles.

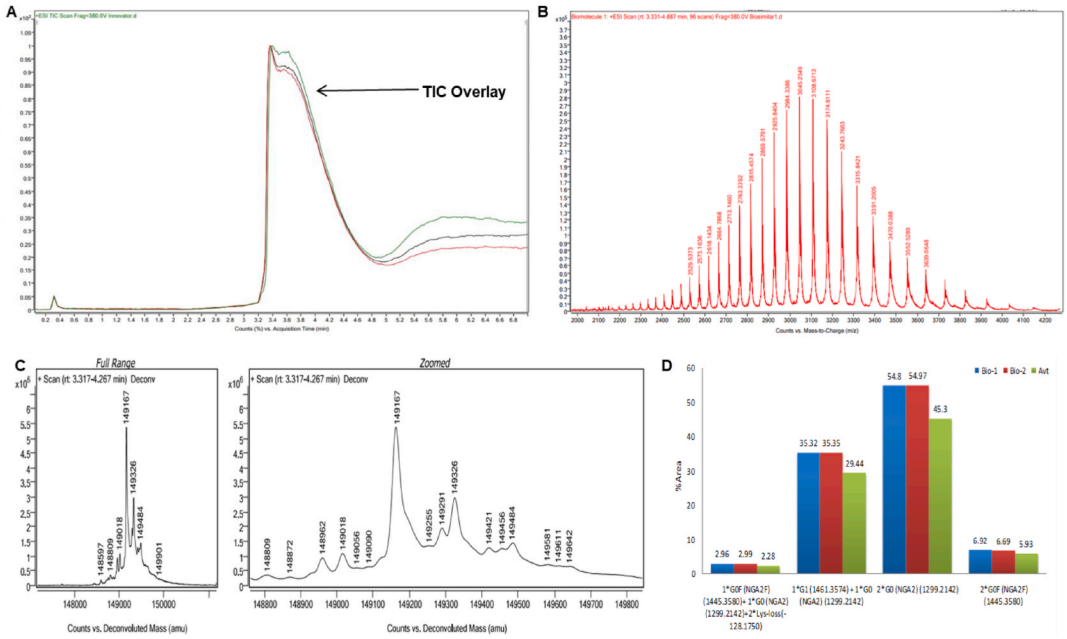

Fig. 2. Intact mass profile of biosimilar formulations and innovator 'Avastin' obtained using UHPLC-ESI-QTOF. (A)Total ion current chromatogram overlay. (B) Summed ion convoluted spectra of Biosimilar-1. (C) Deconvoluted intact mass spectra of Biosimilar-1. (D) Histogram with % area of reported glycoform modifications.

Table 2
Summary of intact mass observed with predicted modifications. *(n = 3)*[a].

Sr. No	Bvz Brand	Rt (min)	Area (%)	Mass (Da)	Tgt. Mass (Da)	Diff (Da)	Predicted Mods
01	Avt	3.628	45.3	149167	149164	+03	2G0 (NGA2) (1299.2142)
02		3.546	29.44	149325	149326	−01	1G1 (1461.3574) + 1G0 (NGA2) (1299.2142)
03		3.546	17.05	149484	149488	−04	2G1 (1461.3574)
04		3.628	5.93	149456	149456	00	2G0F (NGA2F) (1445.3580)
05		3.595	2.28	149056	149054	+02	1G0F (NGA2F) (1445.3580)+ 1G0 (NGA2) (1299.2142)+2Lys-loss (−128.1750)
06	Bio-1	3.380	54.8	149168	149164	+04	2G0 (NGA2) (1299.2142)
07		3.363	35.32	149326	149326	00	1G1 (1461.3574) + 1G0 (NGA2) (1299.2142)
08		3.363	6.92	149458	149456	+02	2G0F (NGA2F) (1445.3580)
09		3.347	2.96	149055	149054	+01	1G0F (NGA2F) (1445.3580)+ 1G0 (NGA2) (1299.2142)+2Lys-loss (−128.1750)
10	Bio-2	3.378	54.97	149168	149164	+04	2G0 (NGA2) (1299.2142)
11		3.378	35.35	149326	149326	00	1G1 (1461.3574) + 1G0 (NGA2) (1299.2142)
12		3.574	6.69	149460	149456	+04	2G0F (NGA2F) (1445.3580)
13		3.378	2.99	149055	149054	+01	1G0F (NGA2F) (1445.3580)+ 1G0 (NGA2) (1299.2142)+2Lys-loss (−128.1750)

[a] **n = 3: Triplicate readings, Rt: Retention time, Tgt mass: Target mass, Diff (Da): Difference in daltons, Mods: modifications.**

structure conformation using FTIR-ATR and CD techniques. Using FTIR-ATR spectroscopy, **seven amide bands** in total are seen in proteins and mAbs. Out of those seven bands, **Amide I bands**; 1617/cm (intermolecular β-sheet), 1635/cm & 1697/cm (antiparallel β-sheet structure), 1668/cm & 1682/cm (β-turns), and 1650/cm (random coils) and **Amide II bands** are particularly relevant to protein and mAb secondary structure characterization. In theory, the Amide I band stands for the **absorptions connected to C = O stretching**, whereas the Amide II band stands for the **absorptions connected to N–H bending**. Both C═O and N–H bonds are involved in the hydrogen bonding between amide and carboxyl functional groups of various amino acids present in the secondary structure of proteins and mAbs [12].

In comparison to the Amide I with Amide II band, **Amide I band is regarded as the more useful predictor** for quantifying the secondary structure of proteins and mAb [13]. The second derivative FTIR-ATR spectrum of Bio-1, Bio-2, and Avt formulations as shown in Fig. 3B confirms the presence of a dominant antiparallel β-sheet structure. For Bio-1, Bio-2, and Avt formulations, similar **FTIR-ATR spectra were observed with peaks at 1617/cm, 1635/cm, 1668/cm, 1670/cm, and 1684/cm**. The **identical pattern confirms that the secondary structure in Bio-1 and Bio-2 formulations were similar to Avt**, which was further supported by the

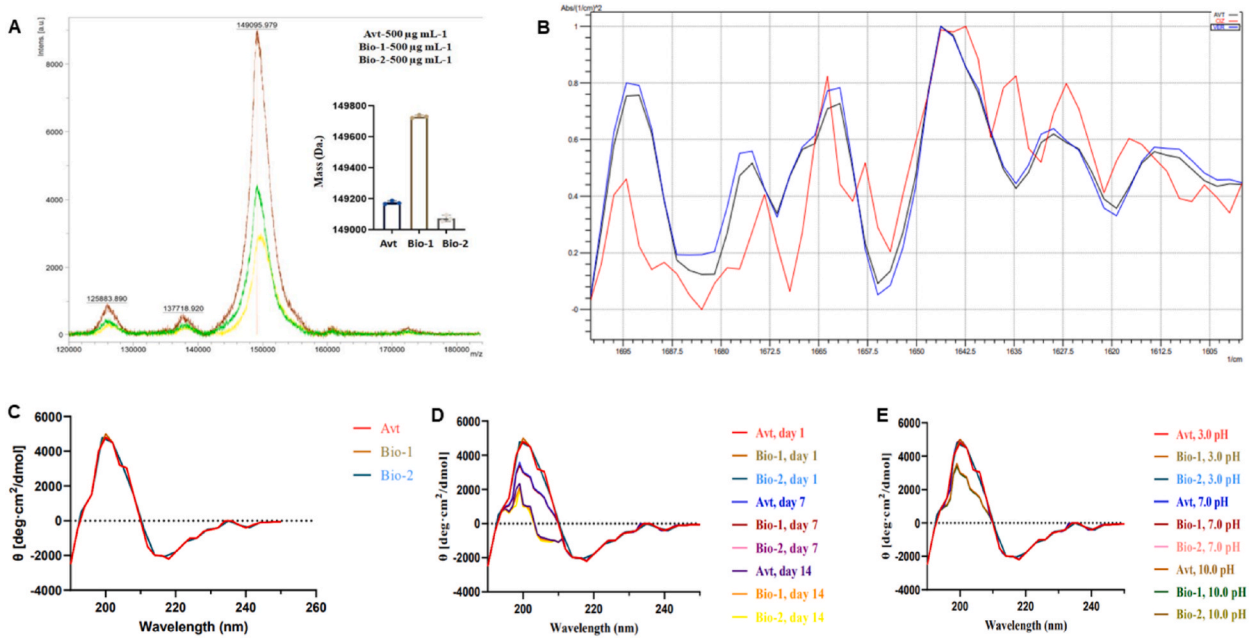

Fig. 3. Qualitative intact mass profile and secondary structure estimation obtained using MALDI-TOF and FTIR-ATR. (A) MALDI-TOF overlay of Bio-1, Bio-2, and Avt formulations. (B) FTIR-ATR overlay of Bio-1, Bio-2, and Avt formulations. (C) CD spectra of Bio-1, Bio-2, and Avt control samples. (D) CD spectra of thermally exposed Bio-1, Bio-2, and Avt samples (E) CD spectra of chemically exposed Bio-1, Bio-2, and Avt samples.

Far-UV CD study. Far UV CD spectra are obtained in the range of 190–250 nm, with a signature peak at 218 nm for Far-UV CD spectra. The intensity of these distinctive peaks revealed the protein's intrinsic structural characteristics and showed through protein folding that these aromatic amino acids and disulfide bonds are present in the chemically inert surrounding [14]. The Far-UV CD study confirms antiparallel β-sheet as the prominent secondary structure of **Bio-1 (40.9 ± 2.0%), Bio-2 (46.5 ± 2.0%) and Avt (44.1 ± 2.0%) control formulations**, Fig. 3C. The Far-UV CD profiles of Bio-1, Bio-2, and Avt control formulations were observed to be **similar and overlapping confirming real time stability**. The effect of **thermal and chemical** stress on Bvz secondary structure conformation responsible for formulation stability was also **evaluated using the Far-UV CD technique. In thermal stress conditions at 50 ± 2°C, over 14 d**, the loss of native antiparallel β-sheet secondary structure was observed with **8.2% loss in Bio-1, 15% loss in Bio-2, and 10.4% loss in Avt** as shown in Fig. 3D. This loss of antiparallel β-sheet conformation in Bvz formulations was joined by an **increase in alternative secondary structure conformations** like **'β-turns' from 18.6% to 24.8%**, as shown in Table 3. Thus, confirming that **deviation in storage temperature leads to the loss of antiparallel β-sheet conformation by 15.0% in Bvz formulations**. Similarly, under chemical stress, throughout 6.0 h, the maximum loss of native antiparallel β-sheet structure was observed in basic condition (0.02 M sodium carbonate-bicarbonate buffer, pH 10 ± 0.2) with **8.3% loss in Bio-1, 11% loss in Bio-2, and 5.6% loss in Avt**, as shown in Fig. 3E and Table 3. In neutral (0.02 M sodium hydrogen phosphate buffer, pH 7.0 ± 0.2), and acidic conditions (0.02 M sodium citrate buffer, pH 3.0 ± 0.2) Far-UV CD **profiles similar to control were observed with no major loss in**

Table 3
Summary of secondary structure modifications observed using *far-UV CD* under thermal and chemical stress conditions. *(n = 3)*.

Stressor condition	Avt				Bio-1				Bio-2			
	Thermal Stress (Temp; 50 ± 2 °C)											
Estimated secondary structure (%)	Ctrl	1 d	7 d	14 d	Ctrl	1 d	7 d	14 d	Ctrl	1 d	7 d	14 d
Helix	0	0	0	2.1	0	0	0	0.6	0	0	0	0
Antiparallel	44.1	38.9	37.9	33.7	44.9	39.5	38.9	32.7	46.5	41.7	36	31.5
Parallel	0	0	0	0	0	0	0	0	0	0	0	0
Turn	18.6	19.8	19.5	26.4	19.8	21.5	24.3	24.8	23.7	19.3	22.4	23.8
Others	37.3	41.3	42.5	37.9	35.3	39	36.8	41.9	29.8	39	41.7	44.7
Stressor condition	Chemical Stress (pH; 3, 7, and 10 for 6 h)											
Estimated secondary structure (%)	Ctrl	Acidic	Neutral	Basic	Ctrl	Acidic	Neutral	Basic	Ctrl	Acidic	Neutral	Basic
Helix	0	0	0	1.6	0	0	0	0	0	0	0	0
Antiparallel	44.2	43.2	44.1	38.6	44.9	43.3	44.8	36.6	46.5	45.4	46.4	35.5
Parallel	0	0	0	0	0	0	0	0	0	0	0	0
Turn	18.5	16.1	18.6	22.3	19.8	16.3	19.9	23.2	23.7	25.4	23.8	24.3
Others	37.3	40.7	37.3	37.5	35.3	40.4	35.3	40.2	29.8	29.2	29.8	40.2

native antiparallel β-sheet conformation. Bar graph showing change in secondary structure (%) of all three thermally and chemically exposed formulations was reported as Fig. S11. Far-UV CD technique proved to be useful for observing the real-time changes occurring in the secondary structure of Bvz formulations. The rapid analysis combined with short and simple sample preparation steps makes it an optimum technique for secondary structure stability evaluation of formulations.

2.3. Size and charge heterogeneity analysis

The real time assessment of **size heterogeneity** was done using **rCE-SDS and nrCE-SDS**. Simultaneously, **charge heterogeneity** was assessed using **iCIEF technique**. The evaluation using CE-SDS was performed under both reduced and non-reduced circumstances. Even though all of the samples were subjected to analysis before their expiration date, there may be discrepancies in purity caused by the samples' varying age. After reducing the Bvz formulations using BME, the heavy chain and light chain (HC−LC) content, non-glycosylated heavy chain (NGHC) content, and LMW and HMW aggregates of Bio-1 and Bio-2 was found to be in accordance with Avt, as shown in Fig. 4A (Figs. S12, S13, S14) and reported as supplementary data (Tables S2–S7). Although after applying one way ANOVA, dunnett's test, significant variation in the % HC content for Avt, Bio-1, and Bio-2 formulations was observed in reduced condition, as shown in Fig. 4B.

No significant difference was observed for % LC content, as shown in Fig. 4C. In non-reduced conditions, intact mAb, LC, NGHC, HMW, and LMW of Bio-1 and Bio-2 formulations were also found to be in accordance with Avt, as shown in Fig. 4D (Figs. S15, S16, S17) and reported in Table S8. After applying dunnett's test no significant variations were observed for % HC and % LC content in non-reduced condition, as shown in Fig. 4E and F. The iCIEF profiles, Fig. 4G, main and acidic species of Bio-1 and Bio-2 were found to be similar to that of Avt. However prominent differences were observed in basic species of biosimilar formulations, which can be due to the presence of C-terminal lysine residue [15]. Further changes in HMW species and NGHC content observed between the formulations were shown in Fig. S18.

2.4. Protein concentration estimation

UV_{280} method profiles were found to be **visually similar** in Bio-1, Bio-2 and Avt formulations, as shown in Fig. 5A. The UV spectrum of mAbs is observed due to the **presence of aromatic amino acids like phenylalanine, tryptophan, and tyrosine** [4]. The mean biosimilarity value of Bio-1 and Bio-2 in comparison to Avt is 98.3% ± 1.5%. The method's **precision limit was set at 95%**. The concentration of Bio-1 and Bio-2 formulations was found to be **24.4–25.1 mg/ml** and **24.3–24.9 mg/ml**, and both were in the preset concentration range of Avt, **24.1–25.3 mg/ml**. Bio-1, Bio-2, and Avt formulations were observed to have high product purity (98.7% ± 0.6%) and similar elution profile using RP-HPLC, as shown in Fig. 5B, C, and 5D.

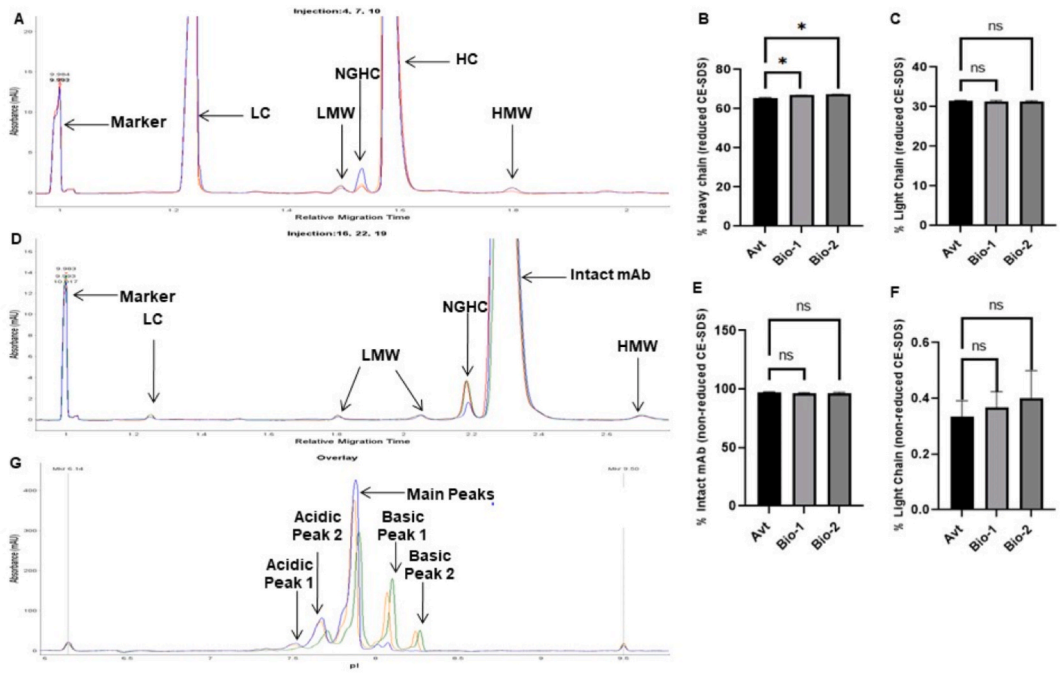

Fig. 4. Size and charge heterogeneity analysis by rCE-SDS, nr-CE-SDS, and iCIEF techniques (A) Overlay of reduced CE-SDS profiles (B) One way ANOVA for % heavy chain in reduced condition (C) One way ANOVA for % light chain in reduced condition (D) Overlay of non-reduced CE-SDS profiles (E) One way ANOVA for % intact mAb in non-reduced condition; (F) One way ANOVA for % light chain in non-reduced condition (G) Overlay of iCIEF profiles.

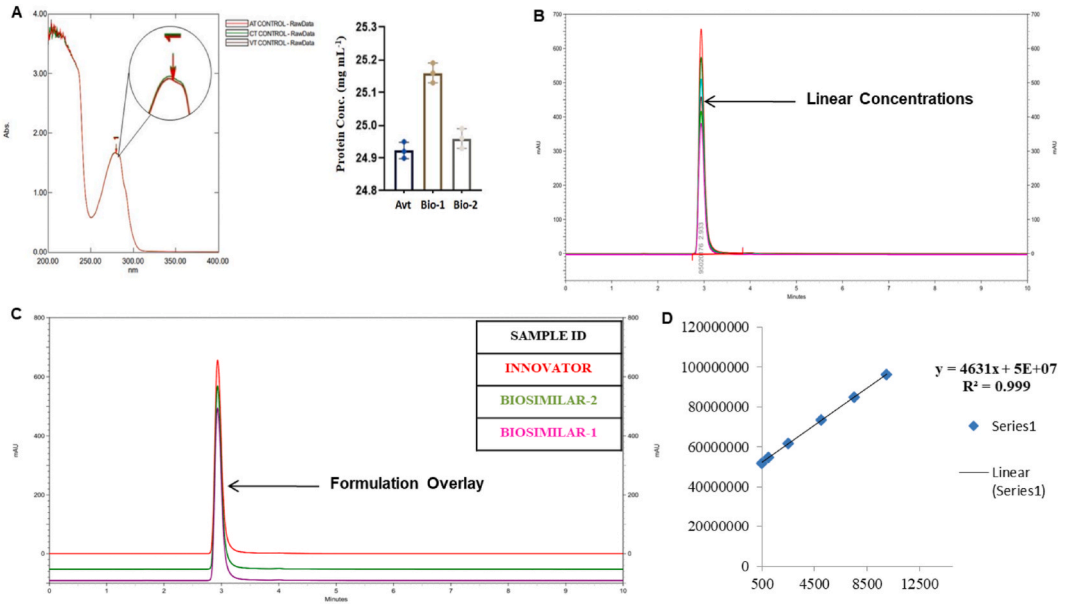

Fig. 5. Protein concentration estimation by UV and RP-HPLC method. (A) UV_{280} overlay with bar graph (B) Chromatogram reporting RP-HPLC method linearity (C) Chromatogram reporting formulation overlay of developed RP-HPLC method (D) Calibration curve of developed RP-HPLC method.

2.5. Aggregate analysis

The **most used chromatographic method** for characterising **macromolecules like mAb** is SEC. Conventional SEC, which employs a single concentration-sensitive detector, might have issues that result inaccurate or even ambiguous information regarding the protein samples being studied. Therefore, the installation of a MALS photometer can expose unsatisfactory separation outcomes in SEC and accurately measure molar mass. Important details on macromolecular size and structure in diluted solution are also provided by MALS. SEC method is most often used to calculate the average and median molar masses of proteins, peptides, and mAbs. **The root-mean-square (RMS) radius, also known as the radius of gyration (Rg) is also measured by the MALS detector**. Intensity at zero

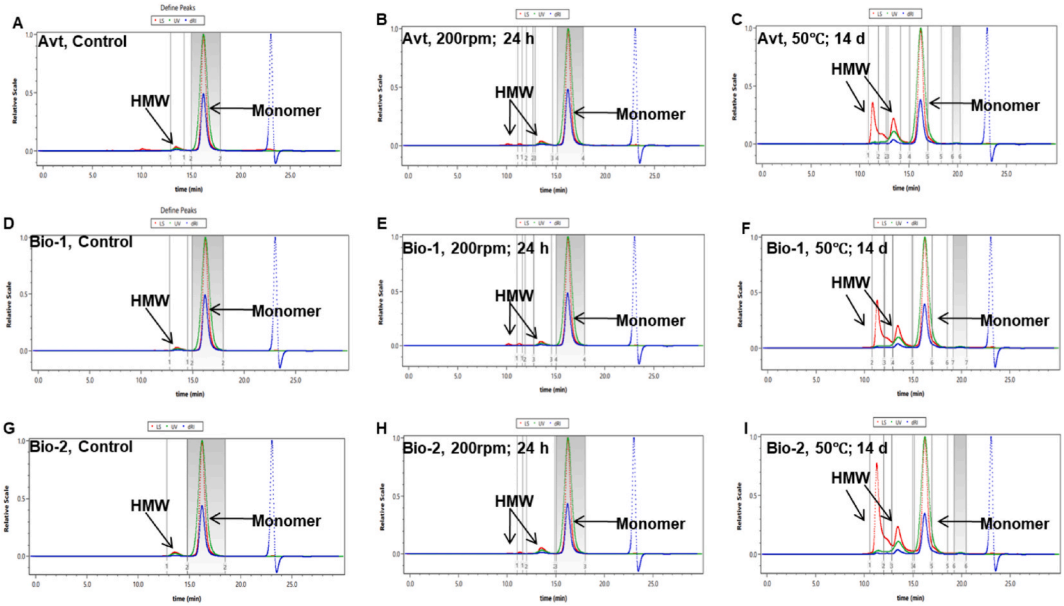

Fig. 6. Aggregate profile obtained using SEC-MALS (A) SEC of Avt control sample (B) SEC of agitated Avt sample; 200 rpm; 24 h. (C) SEC of heated Avt sample; 50 ± 2 °C; 14 d. (D) SEC of Bio-1 control sample. (E) SEC of agitated Bio-1 samples; 200 rpm; 24 h. (F) SEC of heated Bio-1 sample; 50 ± 2 °C; 14 d. (G) SEC of Bio-2 control sample. (H) SEC of agitated Bio-2 samples; 200 rpm; 24 h. (I) SEC of heated Bio-2 sample; 50 ± 2 °C; 14 d.

angle is acquired by extrapolating intensities collected at various angles to zero, and concentration is commonly measured with a differential refractometer (RI detector) in line with the MALS detector. Molar mass is then calculated from these two values. The slope of the angular fluctuation of the dispersed light intensity is used to determine RMS radius. SEC becomes an absolute approach for determining the molar mass distributions of proteins and mAbs with the inclusion of a MALS detector along with the switch to elution-independent analysis [16]. By exposing less-than-ideal SEC separation, MALS also allows you to assess SEC performance objectively. SEC-MALS delivers accurate weight-average molar mass readings even when samples are not well separated. Extremely sensitive detection of ultrahigh-molar-mass species is possible, and this sensitivity is unmatched by conventional RI detection. SEC-MALS analysis prevents the erroneous inferences that may be made from traditional SEC analysis and gives additional details about the structure of mAbs [17,18]. The critical quality attribute (CQA) of product purity, which includes, lot release testing, comparability and similarity assessments are typically assessed using SEC method. However, it is not used to assess protein content as CQA, due to the factors like: sample dilution effect, reversible aggregation process or protein adsorption in chromatographic matrix. All these factors would reduce the quantity of the aggregate and monomeric protein detected [19].

As observed in Fig. 6, chromatographic profiles for Bio-1, Bio-2 and Avt formulations showed HMW aggregates eluting at 11.2 ± 0.2 min, followed by monomer peak at 16.5 ± 0.2 min. **MALS detection module** was then used as an absolute approach to assess the MW (Da) and radius (nm) of control and stressed Bvz formulations. The control Bvz (monomer) formulations reported experimental MW of1.473×10^5 Da (Bio-1), 1.464×10^5 Da (Bio-2), and 1.497×10^5Da (Avt), as shown in Fig. 6A, D, and 6G, and Table 4.

In thermal stress condition (50 ± 2 °C; 1, 7 and 14 d), HMW aggregates started appearing at 7 d in all formulations. The observed HMW aggregate at 7 d corresponds to a trimer with experimental MW of 4.570×10^5 Da (Bio-1), 4.724×10^5 Da (Bio-2), and 4.424×10^5 Da (Avt). Up till 14 d, the MW of aggregates had increased 9 times, 9.313×10^5 Da (Bio-1), 9.853×10^5 Da (Bio-2), and 9.484×10^5 Da (Avt) from the MW of monomer for all formulations, as shown in Fig. 6C, F, 6I, and Table 4.

Simultaneously, the average radius (nm) of monomer and HMW aggregates for all three thermally exposed Bvz formulations changed from 25.3 nm to 13.4 nm and 0.0 nm–23.0 nm, over the course of 14 d. For mechanical stress condition (agitation at 200 rpm; 0, 12, and 24 h), HMW aggregates started appearing after 12 h in all formulations. The observed HMW aggregate after 12 h corresponds to a dimer with experimental MW of 2.832×10^5 Da (Bio-1), 2.982×10^5 Da (Bio-2), and 2.952×10^5 Da (Avt). After 24 h, the MW of aggregates had increased 7 times, 7.107×10^5 Da (Bio-1), 7.726×10^5 Da (Bio-2), and 7.415×10^5 Da (Avt) from the MW of monomer for all formulations, as shown in Fig. 6B, E, 6H, and Table 4.

Simultaneously, the average radius (nm) of monomer and HMW aggregates for all three mechanically stressed Bvz formulations changed from 25.2 nm to 11.6 nm and 0.0 nm–47.5 nm, over the course of 24 h. The average radius of HMW aggregates generated increased in both thermal and mechanical stress conditions by 23.0 nm and 47.5 nm.

The **detection of HMW aggregates** combined with **increasing radius confirms the loss of stability in formulations**. Furthermore, we came to **conclude that HMW aggregates** with large radius get **generated faster in mechanical stress condition**.

SEC technique was found to be **highly effective** for isolating **HMW aggregates** from monomer peak. **MALS detection module** was required to precisely **estimate the MW of Bvz and aggregates generated**. In control Bvz, the MW was observed to be similar for both biosimilar formulations in comparison to the innovator. In thermal and mechanical stress conditions, **aggregates were observed, with increasing MW and radius over time. Confirming that under thermal and mechanical stress conditions,** Bvz undergoes **degradation**, with either **covalent or non-covalent aggregation as major degradation pathway**.

3. Materials and methods

Innovator product, Avastin (Avt, 25 mg/ml, 17 months till expiration), and Biosimilar formulations (Bio-1 & Bio-2, 25 mg/ml each, 18 & 20 months till expiration), were procured from the local retail market of Ahmedabad, Gujarat, India. Milli- Q water, 10 kDa

Table 4
Summary of size heterogeneity and aggregate profile assessed by *SEC-MALS* in thermal and mechanical stress conditions. *(n = 3)*.

Parameter evaluated	Molar mass moments (gm mol^{-1})					
	HMW			Intact mAb		
Bvz Brands	Avt	Bio-1	Bio-2	Avt	Bio-1	Bio-2
Control	nd[a]	nd	nd	1.497×10^5 (±2.598%)	1.473×10^5 (±2.356%)	1.464×10^5 (±2.127%)
50 °C, 1 d	nd	nd	nd	1.498×10^5 (±2.678%)	1.474×10^5 (±2.387%)	1.466×10^5 (±2.237%)
50 °C, 7 d	4.424×10^5 (±3.855%)	4.570×10^5 (±4.163%)	4.724×10^5 (±3.855%)	1.464×10^5 (±2.066%)	1.473×10^5 (±2.045%)	1.495×105 (±2.855%)
50 °C, 14 d	9.484×10^5 (±2.490%)	9.313×10^5 (±2.405%)	9.853×10^5 (±2.450%)	1.495×10^5 (±2.373%)	1.507×10^5 (±2.166%)	1.528×10^5 (±2.449%)
200 rpm, 1 h	nd	nd	nd	1.497×10^5 (±2.578%)	1.473×10^5 (±2.436%)	1.464×10^5 (±2.747%)
200 rpm, 12 h	2.952×10^5 (±2.807%)	2.832×10^5 (±2.627%)	2.982×10^5 (±2.627%)	1.465×10^5 (±2.160%)	1.479×10^5 (±2.531%)	1.485×10^5 (±1.936%)
200 rpm, 24 h	7.415×10^5 (±2.309%)	7.107×10^5 (±2.419%)	7.726×10^5 (±2.229%)	1.445×10^5 (±1.790%)	1.465×10^5 (±2.443%)	1.461×10^5 (±2.720%)

[a] **nd; not detected**.

centrifugal filter units, sodium dihydrogen phosphate, disodium hydrogen phosphate, sodium carbonate, sodium bicarbonate, and sodium citrate were procured from Merck, India. The CE-SDS application kit (P/N PS-MAK03-S), including molecular weight markers, 25× internal standard, 1× sample buffer, and conditioning solutions were purchased from ProteinSimple. The β-mercaptoethanol (BME) (>98% = 14.2 M), iodoacetamide (IAM), and mass-grade sinapinic acid matrix solution were supplied by Merck, India. Mass-grade water, acetonitrile (ACN) and formic acid (FA) were purchased from Honeywell, India.

3.1. Real time stability study using advanced analytical techniques

The real time stability and structural similarity are often controlled by remnants of impurities from the development process. In the reported work, Bio-1 (Mfg: July 2021) and Bio-2 (Mfg: Sept 2021) formulations were compared for real time stability to Avt (Mfg: June 2021) during their shelf life. Sophisticated analytical techniques like electrospray ionization coupled to quadrupole-time of flight mass spectrometer (LC-ESI-QTOF), matrix-assisted laser desorption ionization coupled to time of flight mass spectrometer (MALDI-TOF), Fourier transform infrared spectroscopy (FTIR-ATR), reduced and non-reduced CE-SDS (rCE-SDS, nrCE-SDS), imaged capillary isoelectric focusing (iCIEF), reverse phase high-performance liquid chromatography (RP-HPLC) and (UV_{280}) method were used.

3.2. Forced degradation study using Far-UV CD and SEC-MALS technique

Simultaneously, forced degradation studies were performed in three different stressor conditions. Thermal stress using a stability chamber (the elevated temperature at 50 ± 2 °C) for 1, 7 and 14 d, chemical stress using buffers; acidic pH (3.0 ± 0.2), neutral pH (7.0 ± 0.2), and basic pH (10.0 ± 0.2) for 1, 3 and 6 h, and mechanical stress using dry bath shakers (agitation at 200 rpm) for 1, 12 and 24 h [20]. The effects of thermal and mechanical stress on formulations were assessed by SEC-MALS. To analyze the secondary structure stability of the samples kept under thermal and chemical stress Far-UV CD was used.

3.3. Intact protein analysis by mass spectrometry

AdvanceBio LC6546XT Q-TOF system (Agilent Technologies, Santa Clara, CA, USA) coupled to a Jet Stream ESI source, was used to analyze the molecular mass of intact proteins. Sample separation was done using the 1290 UHPLC system (Agilent Technologies). Bvz biosimilars and innovator samples, 0.5 mg/ml were prepared by performing dilution using 50 mM Tris-HCl pH 7.2. MP consisted of eluting buffer (Buffer B) 0.1% FA in ACN, and loading buffer (Buffer A) 0.1% FA in water. LC separation was performed using PLRP-S column (2.1 mm × 150 mm, 3 μm particle size, 100 Å pore size, Agilent Technologies) at the flow rate of 0.4 ml/min [12]. The elution went from 95% buffer A to 20% buffer A to 95% buffer A within 5.0 min. Acquisition of data was done at a rate of one spectrum/second in the *m/z* range of 500–10,000 and for detailed MS parameters (*See supplementary file for Table S1)*. Using a maximum entropy application incorporated into Agilent Technologies, Mass Hunter software with BioConfirm insert, the resulting summed ion spectra were deconvoluted to yield molecular weight (MW) profiles. Furthermore, the MALDI-TOF study was performed on the Autoflex® Speed instrument (Bruker, Billerica, MA, USA). 20.0 μl of a desalted aliquot from all three Bvz formulations, 25 mg/ml were individually diluted up to 1000 μl using non-ionized water to obtain the final concentration of 0.5 mg/ml. Followed by mixing, 0.5 μl of desalted samples with 0.5 μl of 3, 5-dimethoxy-4-hydroxycinnamic acid (sinapinic acid) matrix. The mixture was spotted on MTP 384 target plate for air drying. Once the sample spot dried, the target plate was then placed inside the MALDI-TOF instrument for intact mass analysis.

3.4. FTIR-ATR for higher order structure characterization

FTIR Spectra were collected using FT/IR-6X (JASCO, Tokyo, Japan) spectrometer in the region of 600–4000/cm. It was equipped with an attenuated total reflectance (ATR) accessory. The spectra were collected at the scan speed of 256 scans/spectra with a resolution of 4/cm. A second derivative spectra smoothening was done using 13 points Savitsky-Golay method. Sample preparation involved a desalting process using 10 KDa, molecular weight cut-off (MWCO) filter units using non-ionized water. Followed by mixing, 160.0 μl aliquot of the desalted sample with 840.0 μl of non-ionized water to achieve a concentration of 4.0 mg/ml which was then transferred to a monolithic diamond crystal.

3.5. rCE-SDS and nrCE-SDS for size heterogeneity analysis

Size heterogeneity analysis by CE-SDS was performed using Maurice (ProteinSimple, San Jose, CA, USA) instrument. Bio-1, Bio-2 and Avt formulations, 2.0 mg/ml were diluted using non-ionized water. To the above-diluted samples (0.8 mg/ml), 2.5 μl IAM solution (250 mM) (alkylation reagent) was added for non-reduced samples or 2.5 μl BME (14.2 M) (reducing reagent) was added for reduced samples followed by thorough mixing using a vortex. Heat the final samples at 70 °C for 10 min using a dry bath or thermocycler. Cool the tube on ice for 5 min followed by the centrifugation process at 1000×*g* using a centrifuge plate adapter. Finally, the samples were transferred to a 96-well plate to be injected into the CE-SDS cartridge.

3.6. iCIEF technique for charge heterogeneity analysis

For charge heterogeneity analysis of Bio-1 and Bio-2 in comparison to Avt, the reported iCIEF method along with the sample

preparation step was used [15]. Using the developed method, the apparent isoelectric point (*pI)* of the formulations as well as the percentage of acidic, neutral and basic species was calculated.

3.7. UV_{280} method for protein concentration estimation

The concentration of all three BVZ formulations was evaluated at 280 nm using a 1900i UV–visible spectrophotometer (Shimadzu, Kyoto, Japan). The theoretical extinction coefficient (ϵ) of 1.66 ml/mg/cm was calculated using the formula $\epsilon 280 = (5500 \times \text{n Trp}) + (1490 \times \text{nTyr}) + (125 \times \text{nS-S})$ which was used for determining samples concentrations.

3.8. RP-HPLC method for protein concentration estimation

1260 Infinity Quaternary LC system (Agilent Technologies) was used for chromatographic analysis. It was equipped with four pumps (G1311C), and a column oven (G1316A). An Agilent G1314F Variable Wavelength Detector (VWD) was attached to the LC module, with a deuterium lamp as a light source and a wavelength range from 190 to 600 nm, respectively. The column used was, Reliant C18 Narrow-bore (4.6 mm × 250 mm, 5 μm particles, 300 Å pore size, Waters, Santa Clara, CA, USA). The chromatographic analysis was carried out using 0.1% FA in 100% water (MP-A) and 0.1% FA in 100% ACN as (MP-B) at a flow rate of 1.0 ml/min. The column oven was kept at 50 °C with detection wavelength set at 280 nm.

3.9. SEC-MALS for protein aggregate analysis in different stressor conditions

Size exclusion chromatography was carried out using the DAWN system (Wyatt Technology, Santa Barbara, CA, USA) incorporated with MALS, UV and RI detectors. The samples kept under thermal and mechanical stress conditions (4 μl) having a concentration of 100 μg/ml were injected into 110 HPLC system (Agilent Technologies) and were separated using TSKgel G3000SWXL mAb HR column (7.8 mm × 300 mm, Tosoh, Tokyo, Japan). The mobile phase used consisted of 300 mM sodium chloride, and 50 mM phosphate buffer (pH 6.7) at a flow rate of 0.5 ml/min. The signal was acquired at the wavelength of 280 nm.

3.10. Far-UV CD for secondary structure analysis in different stressor conditions

The Far-UV CD spectra for all three Bvz formulations were obtained using J-815 CD Spectrpolarimeter (JASCO Corporation). The study was performed for samples kept under thermal stress (50 ± 2 °C) for 1, 7 and 14 d and chemical stress (acidic 3.0 ± 0.2, neutral 7.0 ± 0.2, and basic 10.0 ± 0.2) for 1, 3 and 6 h at the concentration of 0.4 mg/ml. Scans were taken at 25 °C temperature, from 190 to 250 nm range. The bandwidth of 5 nm with 0.1 cm path length, quartz cell, and 50 nm/min scan speed were selected as method parameters. Each sample had three spectra taken, averaged, and then plotted following baseline subtraction.

3.11. Statistical analysis

The statistical analysis was carried out using GraphPad Prism software version 9.2.0. One-way ANOVA, followed by post-hoc dunnett's test, was used to statistically compare the control and group samples. The *p* value greater than 0.5, denotes a significant difference and was used as the parameter.

4. Conclusion

During regular handling as well as in earlier phases of research, development, and manufacturing, biopharmaceuticals get exposed to a wide range of environmental stress conditions. The findings discussed in this paper, focus on real time stability assessment of marketed biosimilar formulations along with aggregate evaluation in above mentioned stress conditions to which bevacizumab biosimilar formulations along with Avastin might get subjected during day-to-day administration. The present study further requires peptide mapping analysis for the identification of post translational modifications occurring due to stress conditions. Similarity was observed between biosimilar marketed formulations and Avastin at all levels of structural characterization. To assess the impact of stress, various stress conditions were selected as already mentioned. The far-UV CD results of these tests indicate that bevacizumab formulations were most affected by high pH condition along with elevated temperature. The basic pH condition and elevated temperature causes mean 11% and 15% loss in native antiparallel β-sheet conformation along with the formation of sulfhydryl, dehydroalanine, D-cysteine, thioether as well as soluble and insoluble aggregates. On the other hand, SEC-MALS results show bevacizumab formulations to be stable when subjected to elevated temperature at 50 ± 2 °C for 1 d only, after that till 14 d increase in the percentage of aggregates was observed with the formation of dimers and trimers. The aggregates formed can be either covalent or non-covalent depending on the factors such as salt and pH of the biosimilar formulations. Regarding the agitation test, significant conformational changes were observed within 24 h, with aggregation being the major degradation pathway. One of the many reported factors responsible for aggregate formation due to agitation is the presence of polysorbate 20 as an excipient in the bevacizumab formulations. Also, methionine and tryptophan have been reported to undergo chemical changes, as a result of increased oxygen transport from vial headspace into the liquid. Therefore, we advise to take great care when handling and transporting the medication and its pharmaceutical preparations, and to avoid shaking them as much as possible. Additionally, care must be exercised when diluting the medication since bevacizumab showed physical changes when exposed to a strongly hypertonic solution. This study therefore, emphasises

the vulnerability of biopharmaceuticals in general and bevacizumab in particular.

Author contribution statement

Arpit Arunkumar Bana: Conceived and designed the experiments; Performed the experiments; Analyzed and interpreted the data; Wrote the paper.

Nithin Sajeev: Performed the experiments; Analyzed and interpreted the data.

Sabyasachi Halder: Analyzed and interpreted the data; Contributed reagents, materials, analysis tools or data.

Haidar Abbas Masi: Analyzed and interpreted the data; Contributed reagents, materials, and analysis tools or data.

Shikha Patel: Analyzed and interpreted the data; Wrote the paper.

Priti Mehta: Conceived and designed the experiments; Analyzed and interpreted the data; Wrote the paper.

Data availability statement

Data will be made available on request.

Additional information

Supplementary content related to this article has been publish online at [URL].

Declaration of competing interest

The authors declare that they have no known competing financial interests or personal relationships that could have appeared to influence the work reported in this paper.

Acknowledgements

We would like to acknowledge Biologics Characterization Facility, C-CAMP Bengaluru, for providing facility to carry out part of the study. We would also like to acknowledge Prof. Chaitanya Joshi <director@gbrc.res.in>and his team at Gujarat Biotechnology and Research Centre (GBRC),Gandhinagar for providing support and access to their facility. Mr. Arpit A. Bana would also like to acknowledge Institute of Pharmacy, Nirma University, Ahmedabad, for providing research fellowship (NU/IP/stipend/Ph.D./2019-2021).

Appendix A. Supplementary data

Supplementary data to this article can be found online at https://doi.org/10.1016/j.heliyon.2023.e19478.

References

[1] C. Nowak, J.K. Cheung, S.M. Dellatore, A. Katiyar, R. Bhat, J. Sun, G. Ponniah, A. Neill, B. Mason, A. Beck, H. Liu, Forced degradation of recombinant monoclonal antibodies: a practical guide, MAbs 9 (2017) 1217–1230, https://doi.org/10.1080/19420862.2017.1368602.

[2] Y. Le Basle, P. Chennell, N. Tokhadze, A. Astier, V. Sautou, Physicochemical stability of monoclonal antibodies: a Review, J. Pharm. Sci. 109 (2020) 169–190, https://doi.org/10.1016/j.xphs.2019.08.009.

[3] K.L. Zapadka, F.J. Becher, A.L. Gomes dos Santos, S.E. Jackson, Factors affecting the physical stability (aggregation) of peptide therapeutics, Interface Focus 7 (2017), https://doi.org/10.1098/rsfs.2017.0030.

[4] A. Martínez-Ortega, A. Herrera, A. Salmerón-García, J. Cabeza, L. Cuadros-Rodríguez, N. Navas, Validated reverse phase HPLC diode array method for the quantification of intact bevacizumab, infliximab and trastuzumab for long-term stability study, Int. J. Biol. Macromol. 116 (2018) 993–1003, https://doi.org/10.1016/j.ijbiomac.2018.05.142.

[5] A.A. Bana, P. Mehta, K.A. Ramnani, Physical instabilities of therapeutic monoclonal antibodies: a critical Review, Curr. Drug Discov. Technol. 19 (2022) 1–11, https://doi.org/10.2174/1570163819666220624092622.

[6] R. Arnon, J. Pikkel, T. Yahalomi, N. Stanescu, K. Wood, A. Leshno, A. Achiron, A. Hilely, The negative impact of COVID-19 pandemic on age-related macular degeneration patients treated with intravitreal bevacizumab injections, Int. Ophthalmol. 42 (2022) 3387–3395, https://doi.org/10.1007/s10792-022-02337-y.

[7] K.B. Shepard, D.T. Vodak, P.J. Kuehl, D. Revelli, Y. Zhou, A.M. Pluntze, M.S. Adam, J.C. Oddo, L. Switala, J.L. Cape, J.M. Baumann, M. Banks, Local treatment of non-small cell lung cancer with a spray-dried bevacizumab formulation, AAPS PharmSciTech 22 (2021) 230, https://doi.org/10.1208/s12249-021-02095-7.

[8] A. Bana, P.J. Mehta, Recognizing barriers to entry of biosimilars in the United States market and highlighting the solutions, J. Generic Med. Bus. J. Generic Med. Sect. 17 (2021) 122–129, https://doi.org/10.1177/1741134320972155.

[9] L. Huang, J. Lu, V.J. Wroblewski, J.M. Beals, R.M. Riggin, In vivo deamidation characterization of monoclonal antibody by LC/MS/MS, Anal. Chem. 77 (2005) 1432–1439, https://doi.org/10.1021/ac0494174.

[10] C. Yu, F. Zhang, G. Xu, G. Wu, W. Wang, C. Liu, Z. Fu, M. Li, S. Guo, X. Yu, L. Wang, Analytical similarity of a proposed biosimilar BVZ-BC to bevacizumab, Anal. Chem. 92 (2020) 3161–3170, https://doi.org/10.1021/acs.analchem.9b04871.

[11] K.A. Brown, S. Rajendran, J. Dowd, D.J. Wilson, Rapid characterization of structural and functional similarity for a candidate bevacizumab (Avastin) biosimilar using a multipronged mass-spectrometry-based approach, Drug Test. Anal. 11 (2019) 1207–1217, https://doi.org/10.1002/dta.2609.

[12] S.K. Singh, D. Kumar, H. Malani, A.S. Rathore, LC–MS based case-by-case analysis of the impact of acidic and basic charge variants of bevacizumab on stability and biological activity, Sci. Rep. 11 (2021) 1–15, https://doi.org/10.1038/s41598-020-79541-2.

[13] Y. Mao, S.G. Valeja, J.C. Rouse, C.L. Hendrickson, A.G. Marshall, Top-down structural analysis of an intact monoclonal antibody by electron capture dissociation-fourier transform ion cyclotron resonance-mass spectrometry, Anal. Chem. 85 (2013) 4239–4246, https://doi.org/10.1021/ac303525n.
[14] L.D. Di Filippo, K.C. dos Santos, G. Hanck-Silva, F.T. de Lima, M.P.D. Gremião, M. Chorilli, A critical Review of biological properties, delivery systems and analytical/bioanalytical methods for determination of bevacizumab, Crit. Rev. Anal. Chem. 51 (2021) 445–453, https://doi.org/10.1080/10408347.2020.1743641.
[15] A. Bana, P. Mehta, Similarity assessment of charge variants for bevacizumab biosimilar formulations using imaged capillary isoelectric focusing, J. Liq. Chromatogr. Relat. Technol. 44 (2021) 801–808, https://doi.org/10.1080/10826076.2022.2072329.
[16] P. Goyal, B. Vats, M. Subbarao, C.G. Honnappa, P. Kabadi, S. Rohil, A. Bera, G.R. Mehta, H. Pai, L. Adhikari, R. Tagore, S. Sharma, R. Venkatachala, P. Nair, S. Annegowda, A. Sahu, S. Trivedi, N. Shastri, Y. Gokhale, R. Thomas, A. Thakur, D. Mohan, U.R. K, R. Melarkode, R. Ullanat, Analytical similarity assessment of MYL-1402O to reference Bevacizumab, Expet. Opin. Biol. Ther. 22 (2022) 271–298, https://doi.org/10.1080/14712598.2021.1973426.
[17] F. Jirjees, K. Soliman, Y. Wang, R. Sonawane, R. Sheshala, D. Jones, R.R.S. Thakur, A validated size exclusion chromatography method coupled with fluorescence detection for rapid quantification of bevacizumab in ophthalmic formulations, J. Pharm. Biomed. Anal. 174 (2019) 145–150, https://doi.org/10.1016/j.jpba.2019.05.038.
[18] A. Oliva, M. Llabrés, Validation of a size-exclusion chromatography method for bevacizumab quantitation in pharmaceutical preparations: application in a biosimilar study, Separations 6 (2019) 1–12, https://doi.org/10.3390/separations6030043.
[19] T. Kaschak, D. Boyd, F. Lu, G. Derfus, B. Kluck, B. Nogal, C. Emery, C. Summers, K. Zheng, R. Bayer, A. Amanullah, B. Yan, Characterization of the basic charge variants of a human IgG1: effect of copper concentration in cell culture media, MAbs 3 (2011) 577–583, https://doi.org/10.4161/mabs.3.6.17959.
[20] J. Kang, T. Halseth, D. Vallejo, Z.I. Najafabadi, K.I. Sen, M. Ford, B.T. Ruotolo, A. Schwendeman, Assessment of biosimilarity under native and heat-stressed conditions: rituximab, bevacizumab, and trastuzumab originators and biosimilars, Anal. Bioanal. Chem. 412 (2020) 763–775, https://doi.org/10.1007/s00216-019-02298-9.